3-1-2019

Deep-ultraviolet laser ablation electrospray ionization mass spectrometry

Remilekun O. Lawal
Louisiana State University

Fabrizio Donnarumma
Louisiana State University

Kermit K. Murray
Louisiana State University

Recommended Citation

Lawal, R., Donnarumma, F., & Murray, K. (2019). Deep-ultraviolet laser ablation electrospray ionization mass spectrometry. *Journal of Mass Spectrometry, 54* (3), 281-287. https://doi.org/10.1002/jms.4338

HHS Public Access

Author manuscript

J Mass Spectrom. Author manuscript; available in PMC 2020 March 01.

Published in final edited form as:

J Mass Spectrom. 2019 March ; 54(3): 281–287. doi:10.1002/jms.4338.

Deep-ultraviolet Laser Ablation Electrospray Ionization Mass Spectrometry

Remilekun O. Lawal, **Fabrizio Donnarumma**, and **Kermit K. Murray***

Department of Chemistry, Louisiana State University, Baton Rouge, Louisiana. 70803, USA

Abstract

A 193 nm wavelength deep ultraviolet laser was used for ambient laser ablation electrospray ionization mass spectrometry of biological samples. A pulsed ArF excimer laser was used to ablate solid samples and the resulting plume of desorbed material merged with charged electrospray droplets to form ions that were detected with a quadrupole time-of-flight mass spectrometer. Solutions containing peptide and protein standards up to 66 kDa molecular weight were deposited on a metal target, dried, and analyzed. No fragmentation was observed from peptides and proteins as well as from the more easily fragmented vitamin B_{12} molecule. The mass spectra contained peaks from multiply-charged ions that were identical to conventional electrospray. Deep UV laser ablation of tissue allowed detection of lipids from untreated tissue. The mechanism of ionization is postulated to involve absorption of laser energy by a fraction of the analyte molecules that act as a sacrificial matrix or by residual water in the sample.

1. Introduction

Ambient mass spectrometry involves the formation of ions outside the mass analyzer without sample preparation.[1–4] Ions are formed when ions or charged droplets impinge on the sample or when a pulsed laser is used to ablate material that then interacts with charge carriers to form ions. Charge to surface ionization can be accomplished using an electrospray ion source directed at a solid sample as with the technique known as desorption electrospray ionization (DESI).[5] Alternatively, ions can be formed by metastable chemical ionization as with direct analysis in real time (DART)[6] when reagent ions are directed at a solid sample. Laser ablation ambient mass spectrometry facilitates removal of sample material from small spots that are a fraction of a millimeter in diameter. The laser ablated material can be directly ionized by infrared laser[7–9] and femtosecond laser matrix-free ionization.[10] An alternative approach is laser post-ionization, a two-step process where the ablation of sample material is followed by post ionization by inductively coupled plasma,[11–13] chemical ionization,[14,15] photoionization,[16] or electrospray ionization.[17–20]

A variety of wavelengths and pulse energies have been used for ambient laser ablation mass spectrometry. An approach called electrospray-assisted laser desorption/ionization (ELDI)

*Corresponding Author and reprint requests: Dr. Kermit K. Murray, 331 Choppin Hall, Department of Chemistry, Louisiana State University, Louisiana, 70803, United States, Phone: +1 (225) 578-3417, Fax: +1 (225) 578 3458, kkmurray@lsu.edu.

Conflict of interest

The authors declare that they have no conflict of interest.

uses a 337 nm pulsed nanosecond nitrogen laser combined with electrospray post-ionization and was the first laser ambient method to detect intact proteins.[18] The matrix-assisted laser desorption electrospray ionization (MALDESI) technique uses a matrix of the type used in matrix-assisted laser desorption ionization (MALDI) to enhance material removal with UV laser ablation.[19] Infrared lasers can be used to ablate material by absorption of vibrational energy by the sample. An early example is the use of a 10.6 μm CO_2 laser to ablate biomolecules for chemical ionization.[14] Mid-IR lasers can be used to excite the OH stretch of water and other compounds containing OH and NH groups. Several configurations have been used to couple nanosecond IR laser ablation with electrospray[21–23] which is most often referred to as laser ablation electrospray ionization (LAESI). Mid-IR lasers has been used with chemical ionization to form a technique known as infrared laser ablation metastable-induced chemical ionization (IR-LAMICI).[24] These mid-IR ablation methods are efficient at ablation of many types of samples using endogenous water as the matrix.

Picosecond and femtosecond lasers have also been used for laser ablation coupled with electrospray ionization. An 800 nm 75 fs pulsed laser was used to ablate material for ionization by electrospray in laser electrospray mass spectrometry (LEMS).[25] The advantage of the fs laser is that it provides efficient ablation without requiring resonant absorption. A 2.88 μm wavelength and 80 ps pulse width a high peak power infrared laser was coupled with electrospray for pulsed infrared laser ablation electrospray ionization (PIR-LAESI).[26]

The use of lasers with wavelengths in the deep ultraviolet region (ca. 200 nm) and beyond for biological mass spectrometry has been reported recently. For example, a Nd:YAG laser fifth harmonic at 213 nm wavelength was used with direct analysis in real time (DART) ionization for ambient mass spectrometry imaging of intact small molecules and metabolites in tissue.[27] Three-dimensional imaging of intact molecules up to 500 *m/z* has also been demonstrated using a 47 nm soft X-ray laser for both desorption and ionization.[28] A 193 nm excimer laser was used for ablation of tissue treated with heavy-metal tagged antibodies and post ionized with inductively coupled plasma mass spectrometry.[29,30] These short wavelength lasers can be focused to small spot sizes for efficient ablation[31] with minimal thermal damage to adjacent areas of the sample.[32] The short wavelength pulses is absorbed by a broad range of compounds. Despite these advantages,[31] deep UV pulsed laser ablation has been limited in application to atoms and small molecules.

In this work, a pulsed nanosecond 193 nm laser was used to demonstrate laser ablation electrospray ionization mass spectrometry of intact biomolecules. Samples were deposited on a metal target held a few millimeters below the inlet of a hybrid quadrupole time-of-flight mass spectrometer with an electrospray emitter held at the same height as the mass spectrometer inlet. The laser ablates material from the sample that is entrained in the cone of the electrospray tip, which results in highly charged molecules. The system was used to demonstrate the detection of intact peptides and proteins from pure compounds and lipids from tissue samples.

2. Material and methods

The configuration used for deep-ultraviolet laser ablation coupled with electrospray is similar to that reported previously for infrared laser ablation;[22] a diagram of the deep ultraviolet laser ablation electrospray ionization (DUVLA-ESI) ion source is shown in Figure 1. A quadrupole time-of-flight mass spectrometer (QSTAR XL, Applied Biosystems, Framingham, MA) was used with the nanoelectrospray ion source and custom spray tip. A 193 nm ArF excimer laser (OPTex, Lambda Physik, Fort Lauderdale, FL) was used at a repetition rate of 5 Hz. The laser was mounted on an optical breadboard adjacent to the ion source. The laser beam was directed onto the sample target using UV fused silica right-angle prisms and was focused with a 10 mm focal length calcium fluoride lens to a 450 × 200 μm spot. A 4 × 1 cm stainless steel sample target was mounted 5 mm below and 4 mm away from the mass spectrometer inlet. The laser incidence angle was 60º from the target surface normal and a laser fluence of 11 kJ/m^2 was used for all experiments unless otherwise indicated. The electrospray emitter was made from a 50 μm ID, 360 μm OD fused silica capillary (Polymicro Technologies, Phoenix, AZ, USA) pulled manually after exposing it to the flame of a butane torch to a ca. 10 μm diameter tip. The tip was placed 8 mm from the mass spectrometer inlet. An equal volume mixture of methanol and water containing 0.1% aqueous trifluoroacetic acid was infused through the capillary at a flow rate of 1 μL/min with a syringe pump (Cole-Parmer, Vernon Hills, IL, USA). A potential of 5.5 kV was applied to the emitter.

Human angiotensin II, bradykinin acetate salt, bovine insulin, cytochrome c from equine heart, hemoglobin, ubiquitin, myoglobin, bovine serum albumin (BSA) and LC-MS grade water were purchased from Sigma-Aldrich (St Louis, MO, USA). Trifluoroacetic acid (99.5%, LC-MS grade) was obtained from Thermo Fisher Scientific (Waltham, MA, USA) and methanol (LC-MS grade) was purchased from EMD Millipore (Burlington, MA, USA). Baseline correction and data point reduction of acquired mass spectra were achieved using a LabVIEW routine. The B-spline algorithm was used to calculate the spectrum baseline while data reduction was achieved by averaging.

Analytes were dissolved in water to a concentration of 1 mg/ml and insulin solutions contained 0.1% TFA to facilitate dissolution. The samples were vortexed until complete dissolution. A 10 μL aliquot of each sample was deposited onto the target by pipette and vacuum dried. For conventional ESI analysis, each solution was further diluted with 1:1 methanol/water 0.1% TFA solution to achieve the desired concentration.

Brain tissue was collected from 6 weeks old rats using procedures approved by the LSU Institutional Animal Care and Use Committee (IACUC) at the LSU School of Veterinary Medicine, Division of Laboratory Animal Medicine (DLAM). The animals were sacrificed via carbon dioxide exposure (5 psi) according to the American Veterinary Medical Association (AVMA) guidelines for the euthanasia of animals. The tissue was removed and immediately frozen with liquid nitrogen. 50 μm thick tissue sections were thaw-mounted on a microscope slide at −20°C using a cryostat (CM 1850, Leica Microsystems, Wetzlar, Germany) and stored at −80°C prior to use. Mounted tissue sections were thawed and vacuum dried for 10min prior to sampling.

3. Results and Discussion

Initial experiments were conducted using peptide standards. Angiotensin II dried droplet samples were ablated at 193 nm and the plume was intercepted by the ESI spray producing spectra with singly and doubly charged ions. The entirety of the sample in the irradiated spot was completely ablated after about 20 laser shots. Mass spectra of angiotensin obtained by UV laser ablation electrospray and conventional electrospray are shown in Figure 2. The mass spectrum in Figure 2a results from a single acquisition mass spectrum of 193 nm ablation of angiotensin II after ca. 5 seconds of laser irradiation. The analyte signal lasted for 3 seconds after the onset of the laser ablation as shown in the total ion signal recorded during the experiment (Figure S1). A conventional electrospray mass spectrum of angiotensin from infusion of a 50 μM angiotensin II solution is shown in Figure 2b. The spectra are similar except for larger Na^+ and K^+ peaks in the DUVLA-ESI mass spectrum. Some nozzle-skimmer fragmentation denoted with asterisks is observed in both spectra. Sample mass spectra could only be obtained with the combination of electrospray and laser. When the laser was operated without the electrospray or the electrospray without the laser, no peaks corresponding to protonated analyte molecules were detected (Figure S1). Experiments using bradykinin peptide were also performed (Figure S2) and confirmed the results obtained with angiotensin II.

Vitamin B_{12} has been used as a thermometer molecule with various ionization techniques.[33–36] Mass spectra of DUVLA-ESI performed on a dried droplet sample of vitamin B_{12} and conventional ESI infusion of the same solution are shown in Figure 3. Figure 3a shows the mass spectrum obtained from ca. 8 nmol of vitamin B_{12} using DUVLA-ESI and Figure 3b show the mass spectrum obtained from infusion of a 50 μM solution of vitamin B_{12}. The base peak is the doubly-protonated molecule in both mass spectra and there is no substantial difference in observed peaks. A peak corresponding to the loss of the cyano group (doubly-charged) was detected in both the DUVLA-ESI and ESI spectra, likely due to nozzle-skimmer dissociation. These results are consistent with those obtained by ESI and infrared laser ablation electrospray of vitamin B_{12}.[37] DUVLA-ESI appears to be as soft an ionization technique as ESI and does not induce fragmentation of vitamin B_{12} as observed with MALDI,[34–36] fast atom bombardment,[38] or plasma desorption mass spectrometry.[39]

Figure 4 shows the spectra of proteins insulin, myoglobin and albumin obtained using DUVLA-ESI from dried droplet samples containing 10 μL of 1mg/ml solution of each protein. All proteins were detected as the multiply protonated intact molecule with no fragmentation detected and no significant difference in the mass spectra compared to conventional electrospray (Figure S3). Figure 4b shows a mass spectrum obtained after ablation of myoglobin. The heme group was detected as a separate singly charged ion. Infusion of 5 μM myoglobin solution (Figure S3) produced a similar spectrum with the heme group lost as well. Similar results with the heme group detected as a singly charged ion has been observed following laser induced desorption and electrospray ionization of myoglobin.[40,41] Results were obtained using protein standards cytochrome c and hemoglobin; their respective spectra are shown in Figure S4.

The DUVLA-ESI approach was further tested using a rat brain tissue section mounted on a microscope slide. Figure 5 shows a representative spectrum obtained from irradiation of an area in the frontal cortex region of the brain. Several peaks between 100 – 900 *m/z* were detected and identified as phospholipids based on searches performed on the Lipid MAPS database[42] using the recorded *m/z*. The dominant peak at *m/z* 760.638 corresponds to protonated PC (34:1) which is a major lipid in rat brain tissue.[43,44] The presence of the peak at *m/z* 577.564 is attributed to the loss of phosphocholine from the PC (34:1). Other prominent protonated ion peaks were observed at *m/z* values of 734.6, 788.6, 806.6, 810.7 and 834.7, corresponding to PC (32:0), PC (36:1), PC (36:6), PC (38:6), and PC (40:6), respectively. The detected phospholipids are consistent with those observed from rat brain tissue using matrix-assisted laser desorption (MALDI)[44] and laser ablation electrospray ionization (LAESI)[17] mass spectrometry. The phosphocholine ion at *m/z* 184.101 is typically detected during collision induced dissociation of phospholipids,[43,44] which further confirms the identity of the detected peaks. This peak is attributed to in source fragmentation in the orifice-skimmer region of the mass spectrometer that induces a CID-like dissociation.[45]

The potential absorbers of the 193 nm irradiation are the analyte, residual water in the sample or tissue, or the sample target. The absorption length of the pure protein (ca. 0.2 μm) and tissue (ca. 1 μm)[46–48] is small compared to the sample thickness (50 μm for tissue and ca. 1 μm for the protein films) which suggests that the sample target does not absorb the laser energy. Further, DUVLA-ESI has been demonstrated with a range of target materials including glass microscope slides with similar results. Proteins have high absorption at 193 nm due to the $\pi \rightarrow \pi^*$ electronic transition of peptide backbone near 190 nm,[48–51] and phosphatidylcholine molecules detected in the DUVLA-ESI analysis of tissue (Figure 5) absorb 193 nm radiation.[52] Thus, the analyte itself may absorb a significant fraction of the laser energy. Whereas the irradiated molecules may fragment, it may be possible that their energy absorption leads to material ejection as a form of “sacrificial matrix”, which has been suggested as a mechanism of IR ablation.[53] Water at room temperature has an absorption coefficient of about 0.1 cm^{-1} at 193 nm, but when heated the peak absorption shifts from its peak at 163 nm to longer wavelengths due to disruption of hydrogen bonding.[54] When heated to a volumetric energy density of 3000 J/m^3 the 193 nm absorption increases to 12,000 cm^{-1}. This effect is similar to the thermal bootstrap effect that has been observed for infrared laser ablation of biomolecules.[55–57] As the system is heated, the absorption increases leading to greater energy absorption. Thus, in addition to analyte absorption, absorption of the laser energy by water may be a factor in the ablation process.

The 8 ns pulse width of the 193 nm laser is shorter than the time for thermal diffusion which is on the microsecond time scale for μm optical penetration depths.[46] In this case, the system is in the thermal confinement regime.[58,59] The system will be in stress confinement if the optical penetration depth is greater than the distance that a pressure wave travels during the laser pulse. The characteristic time for stress confinement is approximately 20 ns in tissue at 193 nm.[46] A large increase in optical absorption at 193 nm due to thermal bootstrap could move the system outside of the pressure confined regime, resulting in less stress in the sample and a less violent ejection of material compared to the infrared. In addition, 193 nm ablation can lead to bond breakage and bubble nucleation from the gases produced by the

photochemical decomposition of the sample.[46] These gases can reduce the effects of phase explosion by providing nucleation sites and reduce the effects of superheating and volumetric boiling. Thus deep-UV ablation can be a physically less violent process compared to mid-IR ablation.

The lack of biomolecule fragmentation observed suggests that the mechanism of material ejection is based on absorption of the laser energy by some of the biomolecules in the sample that photochemically decompose to form gases that serve as nucleation sites for boiling. There may be an additional photothermal component assisted by the strong absorption of water and a UV thermal bootstrap effect. It is likely that the plume of ejected material contains a large quantity of small neutral particulate[60,61] that may efficiently merge with the spray of charged electrospray particles. The low optical penetration depth of the deep UV laser leads to the production of smaller particles than other wavelengths.[62] A large number of small particles formed in this manner would be anticipated to efficiently merge with the electrospray plume in the fused-droplet mechanism proposed for ELDI[18] and LAESI.[21]

Conclusions

Laser ablation coupled with electrospray ionization of peptides and proteins was accomplished using 193 nm deep ultraviolet laser ablation. The biomolecules were observed intact with mass spectra indistinguishable from conventional electrospray. No fragmentation was observed for vitamin B_{12} in contrast to that observed in matrix-assisted laser desorption ionization. Laser ablation electrospray ionization of rat brain tissue at 193 nm allowed the detection of intact phospholipids directly from the sample. The mechanism of ablation is postulated to involve the absorption of laser energy by the analyte molecules themselves or by water in the sample. Absorption by the biomolecules may involve a sacrificial matrix mechanism in which some of the biomolecules absorbing the laser energy are fragmented but the absorbed laser energy expels a large number of intact biomolecules that are ionized and detected. A thermal bootstrap effect that has been previously reported to shift the water electronic absorption into resonance with the 193 nm laser may be an additional component of the laser energy absorption. Deep ultraviolet laser ablation provides opportunities to create ions under ambient conditions with micrometer spatial resolution for mass spectrometry with conventional optics and without the use of a matrix.

Supplementary Material

Refer to Web version on PubMed Central for supplementary material.

Acknowledgements

This work was supported by National institutes of health grant (R21 EB-23110). The authors thank Dr. D. G. Baker (School of Veterinary Medicine, Louisiana State University) for providing rat the brain samples

References

[1]. Cooks RG, Ouyang Z, Takats Z, Wiseman JM. Ambient mass spectrometry. Science 2006, 311, 1566–1570. [PubMed: 16543450]

[2]. Huang M-Z, Yuan C-H, Cheng S-C, Cho Y-T, Shiea J. Ambient ionization mass spectrometry. Annu. Rev. Anal. Chem 2010, 3, 43–65.

[3]. Wu C, Dill AL, Eberlin LS, Cooks RG, Ifa DR. Mass spectrometry imaging under ambient conditions. Mass Spectrom. Rev 2013, 32, 218–243. [PubMed: 22996621]

[4]. Hsu C-C, Dorrestein PC. Visualizing life with ambient mass spectrometry. Curr. Opin. Biotechnol 2015, 31, 24–34. [PubMed: 25146170]

[5]. Takats Z, Wiseman JM, Gologan B, Cooks RG. Mass spectrometry sampling under ambient conditions with desorption electrospray ionization. Science 2004, 306, 471–473. [PubMed: 15486296]

[6]. Cody RB, Laramée JA, Durst HD. Versatile new ion source for the analysis of materials in open air under ambient conditions. Anal. Chem 2005, 77, 2297–2302. [PubMed: 15828760]

[7]. Laiko VV, Baldwin MA, Burlingame AL. Atmospheric pressure matrix-assisted laser desorption/ionization mass spectrometry. Anal. Chem 2000, 72, 652–657. [PubMed: 10701247]

[8]. Laiko VV, Taranenko NI, Berkout VD, Yakshin MA, Prasad CR, Lee HS, Doroshenko VM. Desorption/ionization of biomolecules from aqueous solutions at atmospheric pressure using an infrared laser at 3 μm. J. Am. Soc. Mass. Spectrom 2002, 13, 354–361. [PubMed: 11951973]

[9]. Li Y, Shrestha B, Vertes A. Atmospheric pressure molecular imaging by infrared MALDI mass spectrometry. Anal. Chem 2007, 79, 523–532. [PubMed: 17222016]

[10]. Coello Y, Jones AD, Gunaratne TC, Dantus M. Atmospheric pressure femtosecond laser imaging mass spectrometry. Anal. Chem 2010, 82, 2753–2758. [PubMed: 20210322]

[11]. Gray AL. Solid sample introduction by laser ablation for inductively coupled plasma source mass spectrometry. Analyst 1985, 110, 551–556.

[12]. Russo RE, Mao X, Gonzalez JJ, Mao SS. Femtosecond laser ablation ICP-MS. J. Anal. At. Spectrom 2002, 17, 1072–1075.

[13]. Russo R, Mao X, Gonzalez J, Zorba V, Yoo J. Laser ablation in analytical chemistry. Anal. Chem 2013, 85, 6162–6177. [PubMed: 23614661]

[14]. Coon JJ, McHale KJ, Harrison W. Atmospheric pressure laser desorption/chemical ionization mass spectrometry: a new ionization method based on existing themes. Rapid Commun. Mass Spectrom 2002, 16, 681–685. [PubMed: 11921247]

[15]. Nyadong L, Quinn JP, Hsu CS, Hendrickson CL, Rodgers RP, Marshall AG. Atmospheric pressure laser-induced acoustic desorption chemical ionization mass spectrometry for analysis of saturated hydrocarbons. Anal. Chem 2012, 84, 7131–7137. [PubMed: 22881221]

[16]. Vaikkinen A, Shrestha B, Kauppila TJ, Vertes A, Kostiainen R. Infrared laser ablation atmospheric pressure photoionization mass spectrometry. Anal. Chem 2012, 84, 1630–1636. [PubMed: 22242626]

[17]. Nemes P, Woods AS, Vertes A. Simultaneous imaging of small metabolites and lipids in rat brain tissues at atmospheric pressure by laser ablation electrospray ionization mass spectrometry. Anal. Chem 2010, 82, 982–988. [PubMed: 20050678]

[18]. Shiea J, Huang MZ, HSu HJ, Lee CY, Yuan CH, Beech I, Sunner J. Electrospray-assisted laser desorption/ionization mass spectrometry for direct ambient analysis of solids. Rapid Commun. Mass Spectrom 2005, 19, 3701–3704. [PubMed: 16299699]

[19]. Sampson JS, Hawkridge AM, Muddiman DC. Generation and detection of multiply-charged peptides and proteins by matrix-assisted laser desorption electrospray ionization (MALDESI) Fourier transform ion cyclotron resonance mass spectrometry. J. Am. Soc. Mass. Spectrom 2006, 17, 1712–1716. [PubMed: 16952462]

[20]. Brady JJ, Judge EJ, Levis RJ. Mass spectrometry of intact neutral macromolecules using intense non-resonant femtosecond laser vaporization with electrospray post-ionization. Rapid Commun. Mass Spectrom 2009, 23, 3151–3157. [PubMed: 19714710]

[21]. Nemes P, Vertes A. Laser ablation electrospray ionization for atmospheric pressure, in vivo, and imaging mass spectrometry. Anal. Chem 2007, 79, 8098–8106. [PubMed: 17900146]

[22]. Rezenom YH, Dong J, Murray KK. Infrared laser-assisted desorption electrospray ionization mass spectrometry. Analyst 2008, 133, 226–232. [PubMed: 18227946]

[23]. Sampson JS, Murray KK, Muddiman DC. Intact and top-down characterization of biomolecules and direct analysis using infrared matrix-assisted laser desorption electrospray ionization coupled

to FT-ICR mass spectrometry. J. Am. Soc. Mass. Spectrom 2009, 20, 667–673. [PubMed: 19185512]

[24]. Galhena AS, Harris GA, Nyadong L, Murray KK, Fernández. FM Small molecule ambient mass spectrometry imaging by infrared laser ablation metastable-induced chemical ionization. Anal. Chem 2010, 82, 2178–2181. [PubMed: 20155978]

[25]. Judge EJ, Brady JJ, Barbano PE, Levis RJ. Nonresonant femtosecond laser vaporization with electrospray postionization for ex vivo plant tissue typing using compressive linear classification. Anal. Chem 2011, 83, 2145–2151. [PubMed: 21351794]

[26]. Zou J, Talbot F, Tata A, Ermini L, Franjic K, Ventura M, Zheng J, Ginsberg H, Post M, Ifa DR. Ambient mass spectrometry imaging with picosecond infrared laser ablation electrospray ionization (PIR-LAESI). Anal. Chem 2015, 87, 12071–12079. [PubMed: 26561279]

[27]. Fowble KL, Teramoto K, Cody RB, Edwards D, Guarrera D, Musah RA. Development of “Laser Ablation Direct Analysis in Real Time Imaging” Mass Spectrometry: Application to Spatial Distribution Mapping of Metabolites Along the Biosynthetic Cascade Leading to Synthesis of Atropine and Scopolamine in Plant Tissue. Anal. Chem 2017, 89, 3421–3429. [PubMed: 28234459]

[28]. Kuznetsov I, Filevich J, Dong F, Woolston M, Chao W, Anderson EH, Bernstein ER, Crick DC, Rocca JJ, Menoni CS. Three-dimensional nanoscale molecular imaging by extreme ultraviolet laser ablation mass spectrometry. Nat. Commun 2015, 6, 6944. [PubMed: 25903827]

[29]. Wang HA, Grolimund D, Giesen C, Borca CN, Shaw-Stewart JR, Bodenmiller B, Günther. D Fast chemical imaging at high spatial resolution by laser ablation inductively coupled plasma mass spectrometry. Anal. Chem 2013, 85, 10107–10116. [PubMed: 23957530]

[30]. Giesen C, Wang HA, Schapiro D, Zivanovic N, Jacobs A, Hattendorf B, Schüffler PJ, Grolimund D, Buhmann JM, Brandt S. Highly multiplexed imaging of tumor tissues with subcellular resolution by mass cytometry. Nature Methods 2014, 11, 417. [PubMed: 24584193]

[31]. Geertsen C, Briand A, Chartier F, Lacour J-L, Mauchien P, Sjöström S, Mermet J-M. Comparison between infrared and ultraviolet laser ablation at atmospheric pressure—implications for solid sampling inductively coupled plasma spectrometry. J. Anal. At. Spectrom 1994, 9, 17–22.

[32]. Srinivasan R. Ablation of polymers and biological tissue by ultraviolet lasers. Science 1986, 234, 559–565. [PubMed: 3764428]

[33]. Castro M, Russell D. Cesium ion desorption ionization with Fourier transform mass spectrometry (FTMS). Anal. Chem 1984, 56, 578–581.

[34]. Schiebel HM, Schulten HR. Soft ionization of biomolecules: A comparison of ten ionization methods for corrins and vitamin B12. Mass Spectrom. Rev 1986, 5, 249–311.

[35]. Kinsel GR, Preston LM, Russell DH. Fragmentation of vitamin B12 during 337 nm matrix-assisted laser desorption ionization. Biological mass spectrometry 1994, 23, 205–211.

[36]. He L, Wei G, Murraycor KK. Fragmentation of vitamin B12 in aerosol matrix-assisted laser desorption ionization. J. Am. Soc. Mass. Spectrom 1997, 8, 140–147.

[37]. Nemes P, Huang H, Vertes A. Internal energy deposition and ion fragmentation in atmospheric-pressure mid-infrared laser ablation electrospray ionization. PCCP 2012, 14, 2501–2507. [PubMed: 22249858]

[38]. Barber M, Bordoli RS, Sedgwick RD, Tyler AN. Fast atom bombardment mass spectrometry of cobalamines. Biological Mass Spectrometry 1981, 8, 492–495.

[39]. Blankenship J, VanStipdonk M, Schweikert E. Matrix effects on the fragmentation of vitamin B12 in plasma desorption mass spectrometry. Rapid Commun. Mass Spectrom 1997, 11, 143–147.

[40]. Golovlev V, Allman S, Garrett W, Taranenko N, Chen C. Laser-induced acoustic desorption. Int. J. Mass Spectrom. Ion Processes 1997, 169, 69–78.

[41]. Cheng S-C, Cheng T-L, Chang H-C, Shiea J. Using laser-induced acoustic desorption/electrospray ionization mass spectrometry to characterize small organic and large biological compounds in the solid state and in solution under ambient conditions. Anal. Chem 2008, 81, 868–874.

[42]. Fahy E, Sud M, Cotter D, Subramaniam S. LIPID MAPS online tools for lipid research. Nucleic Acids Res 2007, 35, W606–W612. [PubMed: 17584797]

[43]. Hankin JA, Barkley RM, Murphy RC. Sublimation as a method of matrix application for mass spectrometric imaging. J. Am. Soc. Mass. Spectrom 2007, 18, 1646–1652. [PubMed: 17659880]

[44]. Jackson SN, Wang H-YJ, Woods AS. In situ structural characterization of phosphatidylcholines in brain tissue using MALDI-MS/MS. J. Am. Soc. Mass. Spectrom 2005, 16, 2052–2056. [PubMed: 16253515]

[45]. Schneider BB, Chen DD. Collision-Induced Dissociation of Ions within the Orifice− Skimmer Region of an Electrospray Mass Spectrometer. Anal. Chem 2000, 72, 791–799. [PubMed: 10701264]

[46]. Vogel A, Venugopalan V. Mechanisms of pulsed laser ablation of biological tissues. Chem. Rev 2003, 103, 577–644. [PubMed: 12580643]

[47]. Yablon AD, Nishioka NS, Mikić BB, Venugopalan V. Measurement of tissue absorption coefficients by use of interferometric photothermal spectroscopy. Appl. Opt 1999, 38, 1259–1272. [PubMed: 18305741]

[48]. Fisher BT, Hahn DW. Measurement of small-signal absorption coefficient and absorption cross section of collagen for 193-nm excimer laser light and the role of collagen in tissue ablation. Appl. Opt 2004, 43, 5443–5451. [PubMed: 15508600]

[49]. Dodero VI, Quirolo ZB, Sequeira MA. Biomolecular studies by circular dichroism. Frontiers in Bioscience 2011, 16, 61–73.

[50]. Wetlaufer D. Book Ultraviolet spectra of proteins and amino acids Elsevier 1963 303–390.

[51]. Lembares A, Hu X-H, Kalmus GW. Absorption spectra of corneas in the far ultraviolet region. Invest. Ophthalmol. Vis. Sci 1997, 38, 1283–1287. [PubMed: 9152249]

[52]. Klein DR, Brodbelt JS. Structural characterization of phosphatidylcholines using 193 nm ultraviolet photodissociation mass spectrometry. Anal. Chem 2017, 89, 1516–1522. [PubMed: 28105803]

[53]. Little MW, Laboy J, Murray KK. Wavelength dependence of soft infrared laser desorption and ionization. The Journal of Physical Chemistry 2007, 111, 1412–1416.

[54]. Staveteig PT, Walsh JT. Dynamic 193-nm optical properties of water. Appl. Opt 1996, 35, 3392–3403. [PubMed: 21102727]

[55]. Cramer R, Haglund RF, Jr, Hillenkamp F. Matrix-assisted laser desorption and ionization in the O·H and C·O absorption bands of aliphatic and aromatic matrices: dependence on laser wavelength and temporal beam profile. Int. J. Mass Spectrom. Ion Processes 1997, 169, 51–67.

[56]. Sheffer JD, Murray KK. Infrared matrix-assisted laser desorption/ionization using OH, NH and CH vibrational absorption. Rapid Commun. Mass Spectrom 1998, 12, 1685–1690.

[57]. Menzel C, Dreisewerd K, Berkenkamp S, Hillenkamp F. Mechanisms of energy deposition in infrared matrix-assisted laser desorption/ionization mass spectrometry. Int. J. Mass spectrom 2001, 207, 73–96.

[58]. Zhigilei LV, Garrison BJ. Microscopic mechanisms of laser ablation of organic solids in the thermal and stress confinement irradiation regimes. J. Appl. Phys 2000, 88, 1281–1298.

[59]. Aesa A, Walton C. 193 nm ArF laser ablation and patterning of chitosan thin films. Appl. Phys. A 2018, 124, 444.

[60]. Musapelo T, Murray KK. Particle formation in ambient MALDI plumes. Anal. Chem 2011, 83, 6601–6608. [PubMed: 21797202]

[61]. Cao F, Donnarumma F, Murray KK. Particle size measurement from infrared laser ablation of tissue. Analyst 2016, 141, 183–190. [PubMed: 26630332]

[62]. Apitz I, Vogel A. Material ejection in nanosecond Er: YAG laser ablation of water, liver, and skin. Appl. Phys. A 2005, 81, 329–338.

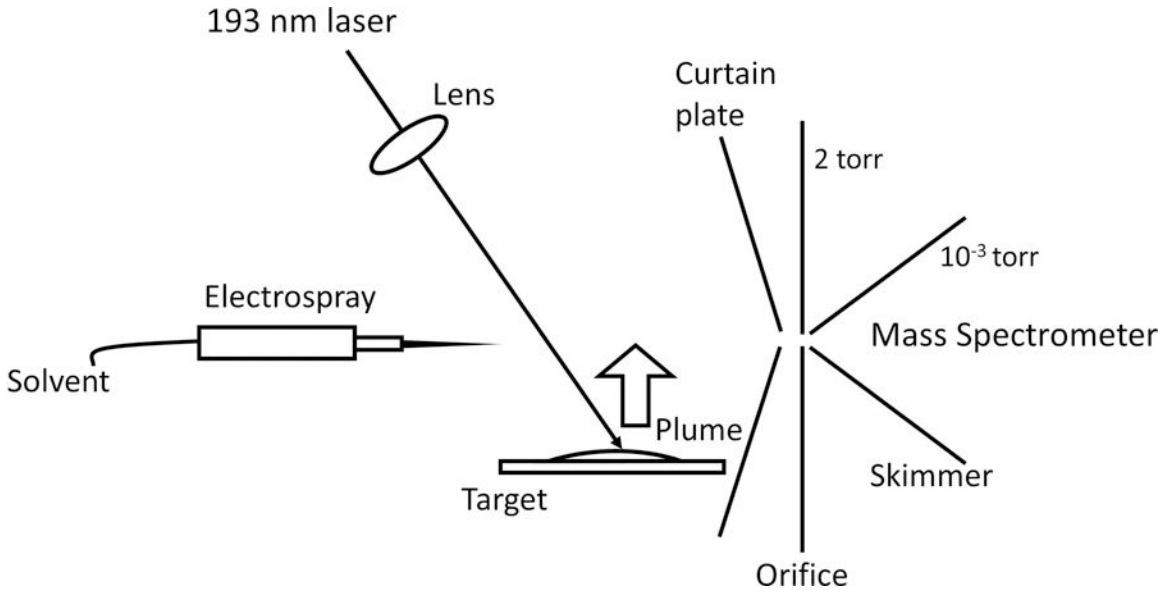

Figure 1.
Schematic of the DUVLA-ESI source: The ES tip is 8 mm away from the MS inlet and 5 mm above the target with the laser focus 4 mm from the tip

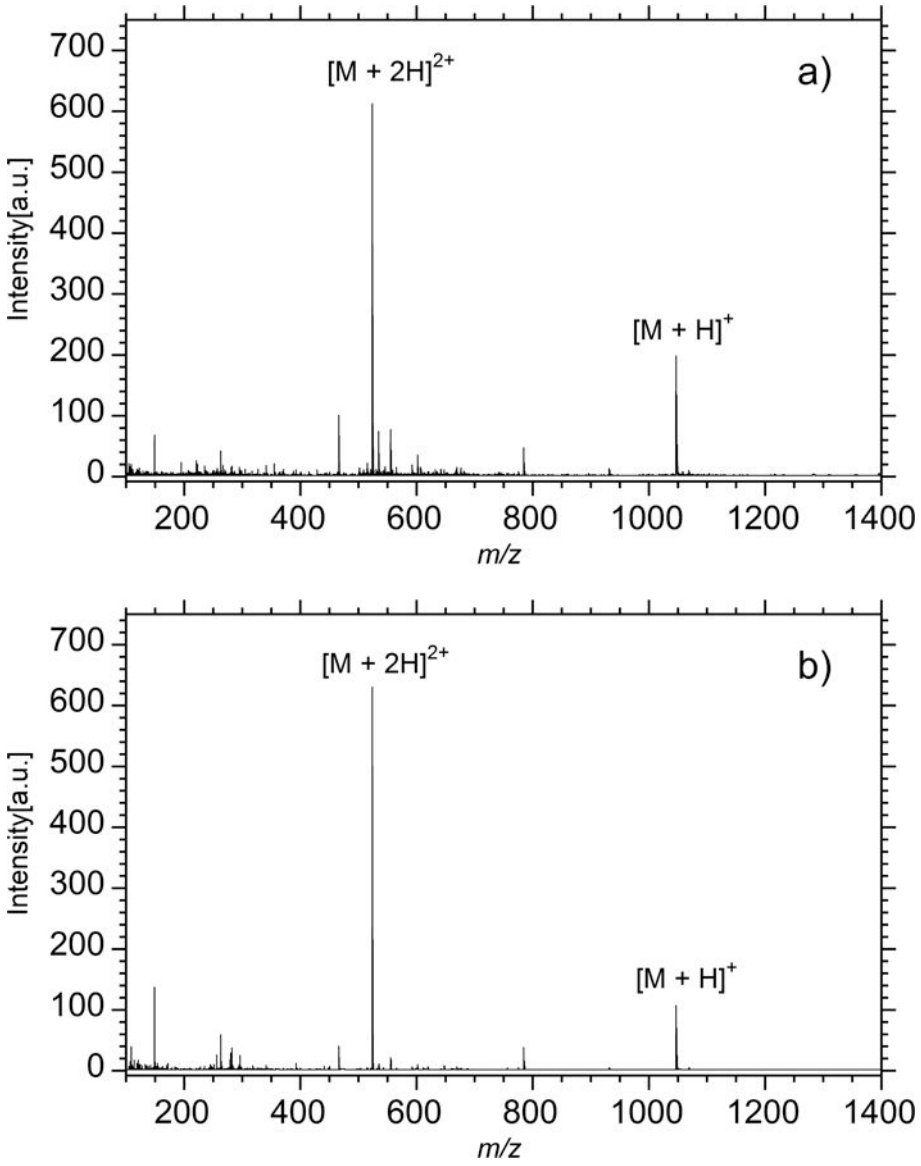

Figure 2.

Mass spectra of angiotensin II acquired with A, 193-nm DUVLA-ESI and B, conventional ESI using a 50-μM angiotensin II solution

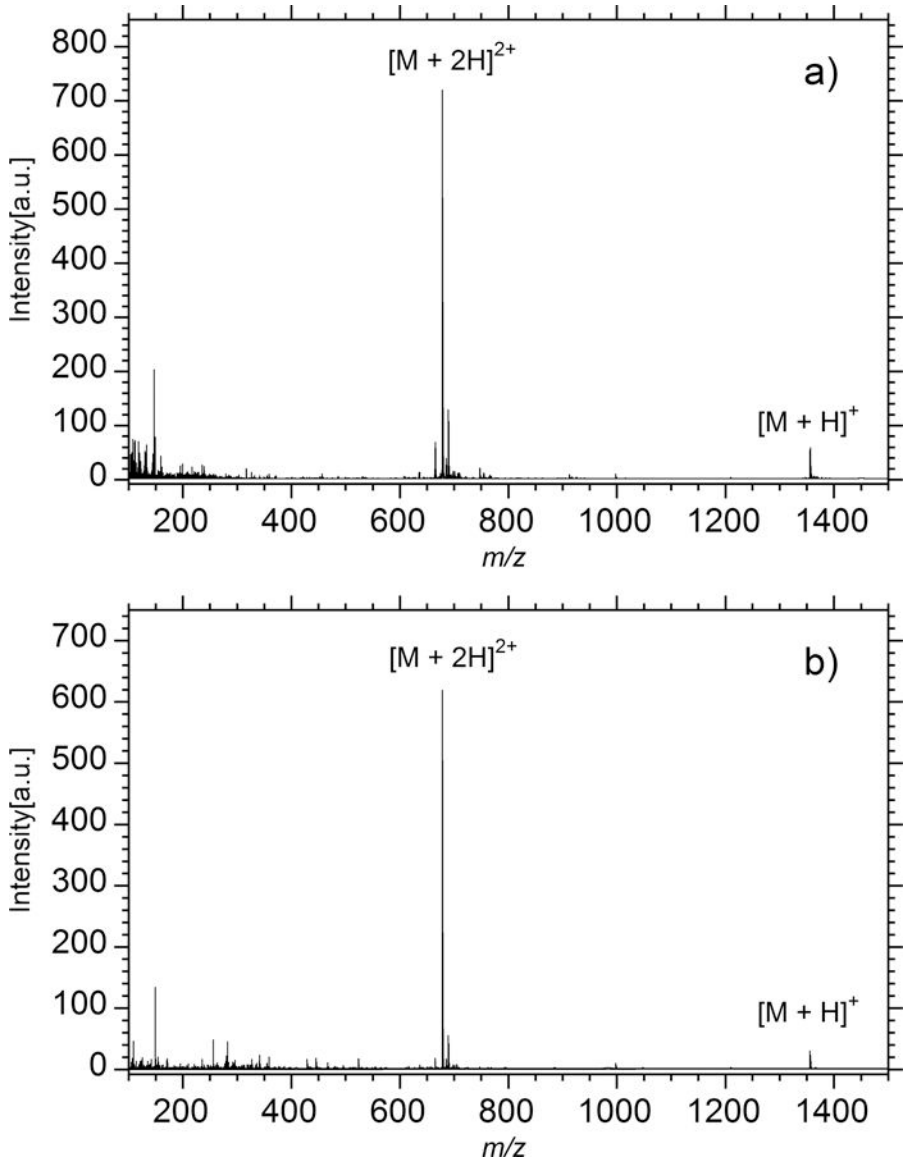

Figure 3.

Mass spectra of vitamin B<sub>12</> acquired with A, 193-nm DUVLA ESI and B, conventional ESI using a 50-μM vitamin B<sub>12</> solution

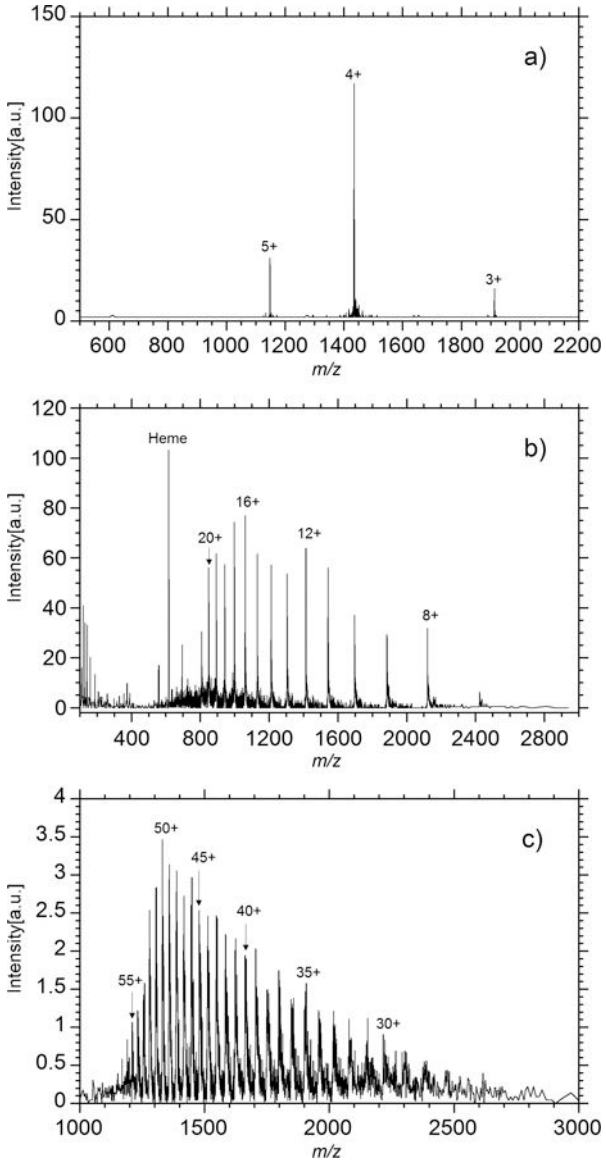

Figure 4.

Mass spectra of A, insulin; B, myoglobin; and C, bovine serum albumin obtained with 193-nm DUVLA ESI

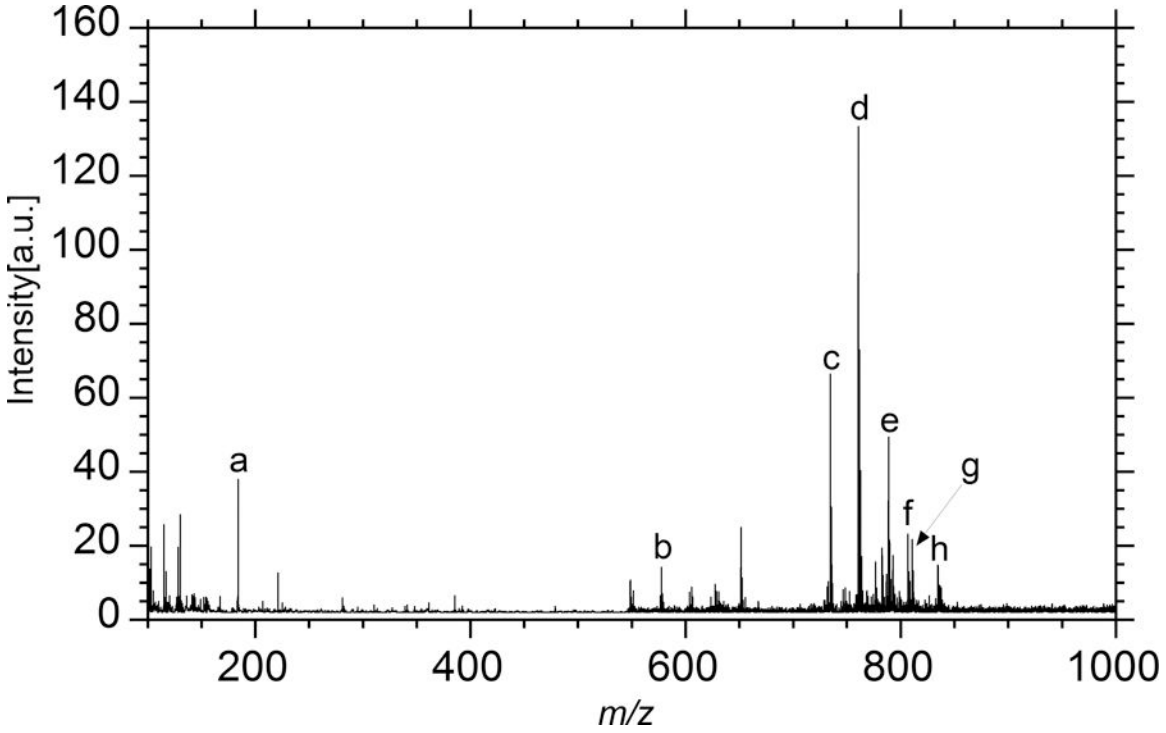

Figure 5.

Representative DUVLA-ESI mass spectrum of a rat brain tissue showing phosphocholine (PC) at m/z 184.1; PC(34:1) fragment at m/z 577.6; PC(32:0) at m/z 734.616; D, PC(34:1) at m/z 760.6; PC(36:1) at m/z 788.6; PC(38:6) at m/z 806.6; PC(38:4) at m/z 810.7; and H, PC(40:6) at m/z 834.7